

Topology and spectral interconnectivities of higher-order multilayer networks

Elkaïoum M. Moutuou,^{1,2,3,*} Obaï B. K. Ali,^{1,2,3,4} and Habib Benali^{1,2,3}

¹PERFORM Centre, Concordia University, Montreal, QC, H4B 1R6

²Gina Cody School of Engineering and Computer Science, Concordia University, Montreal, QC, H3G 1M8

³Department of Electrical and Computer Engineering, Concordia University, Montreal, QC, H3G 1M8

⁴Department of Physics, Concordia University, Montreal, QC, H4B 1R6

Multilayer networks have permeated all the sciences as a powerful mathematical abstraction for interdependent heterogeneous systems such as multimodal brain connectomes, transportation, ecological systems, and scientific collaboration. But describing such complex systems through a purely graph-theoretic formalism presupposes that the interactions that define the underlying infrastructures and support their functions are only pairwise-based; a strong assumption likely leading to oversimplifications. Indeed, most interdependent systems intrinsically involve higher-order intra- and inter-layer interactions. For instance, ecological systems involve interactions among groups within and in-between species, collaborations and citations link teams of coauthors to articles and vice versa, interactions might exist among groups of friends from different social networks, etc. While higher-order interactions have been studied for monolayer systems through the language of simplicial complexes and hypergraphs, a broad and systematic formalism incorporating them into the realm of multilayer systems is still lacking. Here, we introduce the concept of *crosssimplicial multicomplexes* as a general formalism for modelling interdependent systems involving higher-order intra- and inter-layer connections. Subsequently, we introduce *cross-homology* and its spectral counterpart, the *cross-Laplacian* operators, to establish a rigorous mathematical framework for quantifying global and local intra- and inter-layer topological structures in such systems. When applied to multilayer networks, these cross-Laplacians provide powerful methods for detecting clusters in one layer that are controlled by hubs in another layer. We call such hubs spectral cross-hubs (SCH) and define spectral persistence as a way to rank them according to their emergence along the cross-Laplacian spectra. We illustrate our framework through synthetic and empirical datasets.

Keywords: multilayer networks, homology, multicomplexes, laplacian, cross-hubs, spectral persistence

I. INTRODUCTION

Multilayer networks [4, 6, 17] have emerged over the last decade as a natural instrument in modelling myriads of heterogeneous systems. They permeate all areas of science, as they provide a powerful abstraction of real-world phenomena made of interdependent sets of units interacting with each other through various channels. The concepts and computational methods they purvey have been the driving force to recent progress in the understanding of many highly sophisticated structures such as heterogeneous ecological systems [28, 34], spatiotemporal and multimodal human brain connectomes [13, 24, 27], gene-molecule-metabolite interactions [20], and interdisciplinary scientific collaborations [35]. This success has led to a growing interdisciplinary research investigating fundamental properties and topological invariants in multilayer networks.

Some of the major challenges in the analysis of a multilayer network are to quantify the *importance* and *interdependence* among its different components and subsystems, and describe the topological structures of the underlying architecture to better grasp the dynamics and information flows between its different network layers. Various approaches extending concepts, properties, and centrality indices from network science [9, 26] have been developed, leading to tremendous results in many areas of sci-

ence [4, 8, 20, 30, 33, 34, 36, 40]. However, these approaches assume that inter- and intra-communications and relationships between the networks involved in such systems rely solely on node-based interactions. The resulting methods are therefore less insightful when the infrastructure is made up of higher-order *intra-* and *inter-connectivities* among node aggregations from different layers — as it is the case for many phenomena. For example, heterogeneous ecosystems are made up of interactions among groups of the same or different species, social networks often connect groups of people belonging to different circles, collaborations and citations form a higher-order multilayer network made of teams of co-authors interconnected to articles, etc. Many recent studies have explored higher-order interactions and structures in monolayer networks [1–3, 10, 11, 16, 21–23, 31, 32, 37–39] using different languages such as *simplicial complexes* and *hypergraphs*. But a general mathematical formalism for modelling and studying higher-order multilayer networks is still lacking.

Our goal in this study is twofold. First, we propose a mathematical formalism that is rich enough to model and analyze multilayer complex systems involving higher-order connectivities within and in-between their subsystems. Second, we establish a unified framework for studying topological structures in such systems. This is done by introducing the concepts of *crosssimplicial multicomplex*, *cross-homology*, *cross-Betti vectors*, and *cross-Laplacians*. Before we dive deeper into these notions, we shall give the intuition behind them by considering the simple case of an undirected two-layered network Γ ; here Γ consists of two graphs $(V_1, E_1), (V_2, E_2)$,

*Electronic address: elkaïoum.moutuou@concordia.ca

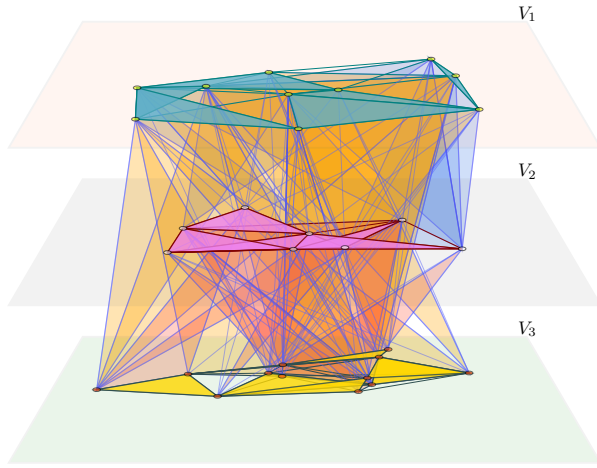


FIG. 1: Schematic of a 2-dimensional crosssimplicial multicomplex \mathcal{X} with 3 layers and 30 nodes in total; \mathcal{X} consists of the vertex sets V_1, V_2, V_3 and the three CSBs $\mathcal{X}^{1,2}, \mathcal{X}^{1,3}, \mathcal{X}^{2,3}$ defined respectively on the products $V_1 \times V_2, V_1 \times V_3$, and $V_2 \times V_3$.

where V_1, V_2 are the node sets of Γ , $E_s \subseteq V_s \times V_s$, $s = 1, 2$ are the sets of intra-layer edges, and a set $E_{1,2} \subseteq V_1 \times V_2$ of *inter-layer edges*. Intuitively, Γ might be seen as a system of interactions between two networks. And what that means is that the node set V_1 interacts not only with V_2 but also with the edge set E_2 and *vice versa*. Similarly, intra-layer edges in one layer interact with edges and triads in the other layer, and so on. This view suggests a more combinatorial representation by some kind of two-dimensional generalization of the fundamental notion of *simplicial complex* from Algebraic Topology [14, 18]. The idea of *crosssimplicial multicomplex* defined in the present work allows such a representation. In particular, when applied to a pairwise based multilayer network, this concept allows to incorporate, on the one hand, the *clique complexes* [19, 31] corresponding to the network layers, and on the other, the clique complex representing the inter-layer relationships between the different layers into one single mathematical object. Moreover, Γ can be regarded through different lenses, and each view displays different kind of topological structures. The most naive perspective flattens the whole structure into a monolayer network without segregating the nodes and links from one layer or the other. Another viewpoint is of two networks with independent or interdependent topologies communicating with each other through the interlayer links. The rationale for defining cross-homology and the cross-Laplacians is to view Γ as different systems each with its own intrinsic topology but in which nodes, links, etc., from one system have some restructuring power that allows them to impose and control additional topologies on the other. This means that in a multilayer system, one layer network might display different topological structures depending on whether we look at it from its own point of view, from the lens of the other layers, or as a part of a whole aggregated structure. We describe this

phenomenon by focusing on the spectra and eigenvectors of the lower degree cross-Laplacians. We shall however remark that our aim here is not to address a particular real-world problem but to provide broader mathematical settings that reveal and quantify the emergence of these structures in any type of multilayer network.

II. CROSSSIMPLICIAL MULTICOMPLEXES

General definitions. Given two finite sets V_1 and V_2 and a pair of integers $k, l \geq -1$, a (k, l) -*crosssimplex* a in $V_1 \times V_2$ is a subset $\{v_0^1, \dots, v_k^1, v_0^2, \dots, v_l^2\}$ of $V_1^{k+1} \times V_2^{l+1}$ where $v_i^s \in V_s$ for $s = 1, 2$. The points v_i^1 (resp. v_j^2) are the *vertices* of a in V_1 (resp. V_2), and its *crossfaces* are its subsets of the form $\{v_0^1, \dots, v_{i-1}^1, v_{i+1}^1, \dots, v_k^1, v_0^2, \dots, v_l^2\}$ for $0 \leq i \leq k$ and $\{v_0^1, \dots, v_k^1, v_0^2, \dots, v_{i-1}^2, v_{i+1}^2, \dots, v_l^2\}$ for $0 \leq i \leq l$. Note that here we have used the conventions that $V_1^n \times V_2^0 = V_1^n$ and $V_1^0 \times V_2^n = V_2^n$.

An *abstract crosssimplicial bicomplex* X (or a CSB) on V_1 and V_2 is a collection of crosssimplices in $V_1 \times V_2$ which is closed under the inclusion of crossfaces; *i.e.*, the crossface of a crosssimplex is also a crosssimplex. A crosssimplex is *maximal* if it is not the crossface of any other crosssimplex. V_1 and V_2 are called the vertex sets of X .

Given a CSB X , for fixed integers $k, l \geq 0$ we denote by $X_{k,l}$ the subset of all its (k, l) -crosssimplices. We also use the notations $X_{0,-1} = V_1$, $X_{-1,0} = V_2$, and $X_{-1,-1} = \emptyset$. And recursively, $X_{k,-1}$ will denote the subset of crosssimplices of the form $\{v_0^1, \dots, v_k^1\} \subset V_1^{k+1}$ and $X_{-1,l}$ as the subset of crosssimplices of the form $\{v_0^2, \dots, v_l^2\} \subset V_2^{l+1}$. Such crosssimplices will be referred to as *intralayer simplices* or *horizontal simplices*. We then obtain two simplicial complexes [14] $X_{\bullet,-1}$ and $X_{-1,\bullet}$, that we will refer to as the *intralayer complexes*, and whose vertex sets are respectively V_1 and V_2 . In particular, $X_{1,-1}$ and $X_{-1,1}$ are graphs with vertex sets V_1 and V_2 , respectively.

The *dimension* of a (k, l) -crosssimplex is $k + l + 1$, and the dimension of the CSB X is the dimension of its crosssimplices of highest dimension. The n -*skeleton* of X is the restriction of X to the (k, l) -crosssimplices such that $k + l + 1 \leq n$. In particular, the 1-skeleton of a CSB is a 2-layered network, with $X_{0,0}$ being the set of interlayer links. Conversely, given a 2-layered network Γ formed by two graphs $\Gamma_1 = (V_1, E_1)$, $\Gamma_2 = (V_2, E_2)$ with interlayer edge set $E_{1,2} \subset V_1 \times V_2$, define a (k, l) -*clique* in Γ as a pair (σ_1, σ_2) where σ_1 is a k -clique in Γ_1 and σ_2 is an l -clique in Γ_2 with the property that $(i, j) \in E_{1,2}$ for every $i \in \sigma_1$ and $j \in \sigma_2$. We define the *cross-clique bicomplex* X associated to Γ by letting $X_{k,l}$ to be the set of all $(k + 1, l + 1)$ -cliques in Γ .

Now a *crosssimplicial multicomplex* (CSM) \mathcal{X} consists of a family of finite sets V_s , $s \in S \subseteq \mathbb{N}$, and a CSB $\mathcal{X}^{s,t}$ for each pair of distinct indices $s, t \in S$. It is *undirected* if the sets of crosssimplices in $\mathcal{X}^{s,t}$ and $\mathcal{X}^{t,s}$ are in one-to-one correspondence. In such a case, \mathcal{X} is completely defined by the family of CSB $\mathcal{X}^{s,t}$ with $s < t$ (see Fig. 1 for a visualization of a 3-layer CSM).

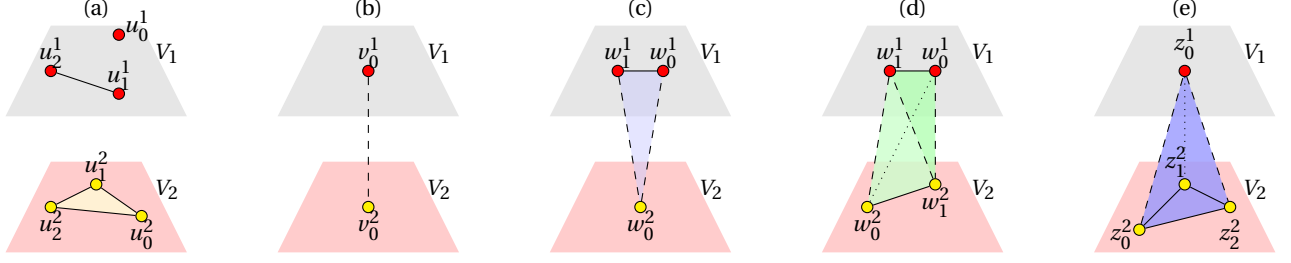


FIG. 2: **Crosssimplices.** Schematic of: (a) A $(0, -1)$ -crosssimplex (a top vertex), a $(1, -1)$ -crosssimplex (top horizontal edge), and a $(-1, 2)$ -crosssimplex (bottom horizontal triangle); (b) a $(0, 0)$ -crosssimplex (a cross-edge); (c) a $(1, 0)$ -crosssimplex (a top cross-triangle); (d) a $(1, 1)$ -crosssimplex (a cross-tetrahedron); and (e) a $(0, 2)$ -crosssimplex (also a cross-tetrahedron). Notice that cross-edges are always oriented from the vertex of the top layer to the one in the bottom layer. Therefore, cross-edges belonging to a cross-triangle are always of opposite orientations with respect to any orientation of the cross-triangle. There are two types of cross-triangles: the $(1, 0)$ -crosssimplices (top cross-triangles) and the $(0, 1)$ -crosssimplices (the bottom cross-triangle). Moreover, there are three types of cross-tetrahedrons: the $(0, 2)$ -crosssimplices, the $(2, 0)$ -crosssimplices, and the $(1, 1)$ -crosssimplices.

Orientation on crosssimplices. An *orientation* of a (k, l) -crosssimplex is an ordering choice over its vertices. When equipped with an orientation, the crosssimplex is said to be *oriented* and will be represented as $[a] = [v_0^1, \dots, v_k^1; v_0^2, \dots, v_l^2]$ if $k, l \geq 0$, or $[v_0^1, \dots, v_k^1]$ (resp. $[v_0^2, \dots, v_l^2]$) if $k \geq 0$ and $l = -1$ (resp. $k = -1$ and $l \leq 0$). We shall note that an orientation on crosssimplices is just a choice purely made for computational purposes. Extending geometric representations from simplicial complexes, crosssimplices can be represented as geometric objects. Specifically, a $(0, -1)$ -crosssimplex is a vertex in the top layer; $(0, 0)$ -crosssimplex is a *cross-edge* between layers V_1 and V_2 ; a $(1, -1)$ -crosssimplex (resp. $(-1, 1)$ -crosssimplex) is a *horizontal edge* on V_1 (resp. V_2); a $(0, 1)$ -crosssimplex or a $(1, 0)$ -crosssimplex is a *cross-triangle*; a $(2, -1)$ -crosssimplex or $(-1, 2)$ -crosssimplex is a *horizontal triangle* on layer V_1 or V_2 ; a $(3, -1)$ -crosssimplex or $(-1, 3)$ -crosssimplex is a *horizontal tetrahedron* on V_1 or V_2 ; a $(1, 1)$ -crosssimplex, a $(2, 0)$ -crosssimplex, or a $(0, 2)$ -crosssimplex, is a *cross-tetrahedron*; and so on (see Fig. 2 for illustrations). On the other hand, *horizontal edges*, triangles, tetrahedron, and so on, are just usual simplices on the horizontal complexes. One can think of a cross-edge as a connection between a vertex from one layer to a vertex on the other layer. In the same vein, a cross-triangle can be thought of as a connection between one vertex from one layer and two vertices on the other, and a cross-tetrahedron as a connection between either two vertices from one layer and two vertices on the other, or one vertex from one layer to three vertices on the other.

Weighted CSBs. A *weight* on a CSB X is a positive function $w : \bigcup_{k,l} X_{k,l} \rightarrow \mathbb{R}^+$ that does not depend on the orientations of crosssimplices. A *weighted CSB* is one that is endowed with a weight function. The *weight of a crosssimplex* $a \in X$ is the number $w(a)$.

III. TOPOLOGICAL DESCRIPTORS

Cross-boundaries. A CSB X defines a *bisimplicial set* [12, 25] by considering respectively the *top* and *bottom crossface maps* $d_{i|k,l}^{(1)} : X_{k,l} \rightarrow X_{k-1,l}$ and $d_{i|k,l}^{(2)} : X_{k,l} \rightarrow X_{k,l-1}$ by

$$\begin{aligned} d_{i|k,l}^{(1)}([v_0^1, \dots, v_k^1; v_0^2, \dots, v_l^2]) &= [v_0^1, \dots, \widehat{v_i^1}, \dots, v_k^1; v_0^2, \dots, v_l^2] \\ d_{i|k,l}^{(2)}([v_0^1, \dots, v_k^1; v_0^2, \dots, v_l^2]) &= [v_0^1, \dots, v_k^1; v_0^2, \dots, \widehat{v_i^2}, \dots, v_l^2] \end{aligned} \quad (1)$$

where the hat over a vertex means dropping the vertex. Moreover, for a fixed $l \geq -1$, $X_{\bullet,l} = (X_{k,l})_{k \geq -1}$ is a simplicial complex. Similarly, $X_{k,\bullet} = (X_{k,l})_{l \geq -1}$ is a simplicial complex. Observe that if $a = \{v_0^1, \dots, v_k^1, v_0^2, \dots, v_l^2\} \in X_{k,l}$, then $a^{(1)} = \{v_0^1, \dots, v_k^1\} \in X_{k,-1}$ and $a^{(2)} = \{v_0^2, \dots, v_l^2\} \in X_{-1,l}$. We will refer to $a^{(1)}$ and $a^{(2)}$ as *the top horizontal face* and *the bottom horizontal face* of a , respectively. Conversely, two horizontal simplices $v^1 \in X_{k,-1}$ and $v^2 \in X_{-1,l}$ are said to be *interconnected* in X if they are respectively the top and bottom horizontal faces of a (k, l) -crosssimplex a . We then write $v^1 \sim v^2$. This is basically equivalent to requiring that if $v^1 = \{v_0^1, \dots, v_k^1\}$ and $v^2 = \{v_0^2, \dots, v_l^2\}$ then $\{v_0^1, \dots, v_k^1, v_0^2, \dots, v_l^2\} \in X_{k,l}$. If $a = \{v_0^1, \dots, v_k^1, v_0^2, \dots, v_l^2\} \in X_{k,l}$, we define its *top cross-boundary* $\partial^{(1)} a$ as the subset of $X_{k-1,l}$ consisting of all the top crossfaces of a ; i.e., all the $(k-1, l)$ -crosssimplices of the form $d_{i|k,l}^{(1)}[a]$ for $i = 0, \dots, k$. Analogously, its *bottom cross-boundary* $\partial^{(2)} a \subseteq X_{k,l-1}$ is the subset of all its bottom crossfaces $d_{i|k,l}^{(2)}[a]$, $i = 0, \dots, l$.

Now two (k, l) -crosssimplices $a, b \in X_{k,l}$ are said to be:

- *top-outer (TO) adjacent*, and we write $a \frown^{(1)} b$ or $a \frown_c^{(1)} b$, if both are top crossfaces of a $(k+1, l)$ -crosssimplex c ; in other words $a, b \in \partial^{(1)} c$;
- *top-inner (TI) adjacent*, and we write $a \smile_{(1)} b$ or $a \smile_{(1)}^d b$, if there exists a $(k-1, l)$ -crosssimplex $d \in X_{k-1,l}$ which is a top crossface of both a and b ; i.e., $d \in \partial^{(1)} a \cap \partial^{(1)} b$;
- *bottom-outer (BO) adjacent*, and we write $a \frown^{(2)} b$ or

$a \frown_c^{(2)} b$, if both are bottom crossfaces of a $(k, l+1)$ -crosssimplex $c \in X_{k, l+1}$; that is to say $a, b \in \partial^{(2)} c$; and

- *bottom-inner (BI) adjacent*, and we write $a \smile_{(2)}^{(2)} b$ or $a \smile_{(2)}^d b$, if there exists a $(k, l-1)$ -crosssimplex $f \in X_{k, l-1}$ which is a bottom face of both a and b ; that is $d \in \partial^{(2)} a \cap \partial^{(2)} b$.

Degrees of crosssimplices. Given a weight function w on X , we define the following degrees of a (k, l) -crosssimplex a relative to w .

- The *TO degree* of a is the number

$$\deg_{TO}(a) = \deg_{TO}(a, w) := \sum_{\substack{a' \in X_{k+1, l} \\ a \in \partial^{(1)} a'}} w(a'). \quad (2)$$

- Similarly, the *TI degree* of a is defined as

$$\deg_{TI}(a) = \deg_{TI}(a, w) := \sum_{\substack{c \in X_{k-1, l} \\ c \in \partial^{(1)} a}} \frac{1}{w(c)}. \quad (3)$$

- Analogously, the *BO degree* of a is given by

$$\deg_{BO}(a) = \deg_{BO}(a, w) := \sum_{\substack{a' \in X_{k, l+1} \\ a \in \partial^{(2)} a'}} w(a'). \quad (4)$$

- And the *BI degree* of a is

$$\deg_{BI}(a) = \deg_{BI}(a, w) := \sum_{\substack{c \in X_{k, l-1} \\ c \in \partial^{(2)} a}} \frac{1}{w(c)}. \quad (5)$$

Observe that in the particular case where the weight function is everywhere equal to one, the TO degree of a is precisely the number of $(k+1, l)$ -crosssimplices in X of which a is top cross-face, while $\deg_{TI}(a)$ is the number of top cross-faces of a , which equals to $k+1$. Analogous observation can be made about the BO and BI degrees.

Cross-homology groups. Define the space $C_{k, l}$ of (k, l) -cross-chains as the real vector space generated by all oriented (k, l) -crosssimplices in \mathcal{X} . The *top* and *bottom cross-boundary operators* $\partial_{k, l}^{(1)} : C_{k, l} \rightarrow C_{k-1, l}$, $\partial_{k, l}^{(2)} : C_{k, l} \rightarrow C_{k, l-1}$ are then defined as follows by the formula

$$\partial_{k, l}^{(s)}([a]) := \sum_{b \in \partial^{(s)} a} \text{sgn}(b, \partial^{(s)} a)[b], \quad (6)$$

for $s = 1, 2$ and a generator $a \in X_{k, l}$, where $\text{sgn}(b, \partial^{(s)} a)$ is the sign of the orientation of b in $\partial^{(s)} a$; that is, if $b = d_{i|k, l}^{(1)}[a]$, then $\text{sgn}(b, \partial^{(1)} a) := (-1)^i$, and we define $\text{sgn}(b, \partial^{(2)} a)$ in a similar fashion.

It is straightforward to see that in particular

$$\partial_{k-1}^{(1)} : C_{k-1} \rightarrow C_{k-1, -1}, \quad k \geq 0,$$

and

$$\partial_{-1, l}^{(2)} : C_{-1, l} \rightarrow C_{-1, l}, \quad l \geq 0$$

are the usual boundary maps of simplicial complexes. For this reason, we will put more focus on the mixed case where both l and k are non-negative. We will often drop the indices and just write $\partial^{(1)}$ and $\partial^{(2)}$ to avoid cumbersome notations. To see how these maps operates, let us compute for instance the images of the crosssimplices (b), (c), (d) and (e) illustrated in Fig. 2. We get:

$$\begin{cases} \partial_{0,0}^{(1)}[v_0^1; v_0^2] = [v_0^2] \in C_{-1,0} \\ \partial_{0,0}^{(2)}[v_0^1; v_0^2] = -[v_0^1] \in C_{0,-1}; \end{cases}$$

$$\begin{cases} \partial_{1,0}^{(1)}[w_0^1, w_1^1; w_0^2] = [w_1^1; w_0^2] - [w_0^1; w_0^2] \in C_{0,0}, \\ \partial_{1,0}^{(2)}[w_0^1, w_1^1; w_0^2] = [w_0^1, w_1^1] \in C_{1,-1}; \end{cases}$$

$$\begin{cases} \partial_{1,1}^{(1)}[w_0^1, w_1^1; w_0^2, w_1^2] = [w_1^1; w_0^2, w_1^2] - [w_0^1; w_0^2, w_1^2] \in C_{0,1}, \\ \partial_{1,1}^{(2)}[w_0^1, w_1^1; w_0^2, w_1^2] = [w_0^1, w_1^1; w_1^2] - [w_0^1, w_1^1; w_0^2] \in C_{1,0}; \end{cases}$$

$$\begin{cases} \partial_{0,2}^{(1)}[z_0^1, z_0^2, z_1^2, z_2^2] = [z_0^2, z_1^2, z_2^2] \in C_{-1,2} \\ \partial_{0,2}^{(2)}[z_0^1, z_0^2, z_1^2, z_2^2] = [z_0^1; z_1^2, z_2^2] - [z_0^1; z_0^2, z_2^2] \\ \quad + [z_0^1; z_0^2, z_1^2] \in C_{0,1}. \end{cases}$$

Notice that $\partial_{0,-1}^{(1)} = \partial_{-1,0}^{(2)} = 0$. Moreover, by simple calculations from (6), it is easy to check that $\partial_{k-1, l}^{(1)} \partial_{k, l}^{(1)} = 0$ and $\partial_{k, l-1}^{(2)} \partial_{k, l}^{(2)} = 0$, which allows to define the *top* and *bottom* (k, l) -cross-homology groups of X as the quotients

$$H_{k, l}^{(1)}(X) := \ker \partial_{k, l}^{(1)} / \text{im } \partial_{k+1, l}^{(1)}, \quad \text{and}$$

$$H_{k, l}^{(2)}(X) := \ker \partial_{k, l}^{(2)} / \text{im } \partial_{k, l+1}^{(2)}.$$

For $k \geq 0$ and $l \leq 0$, $\partial_{k-1}^{(1)}$ and $\partial_{-1, l}^{(2)}$ are the usual boundary maps of simplicial complexes [14]. Therefore $H_{k-1}^{(1)}(X)$ and $H_{-1, l}^{(2)}(X)$ are the usual homology groups [14, 18] of the simplicial complexes $X_{\bullet, -1}$ and $X_{-1, \bullet}$, respectively.

Cross-Betti vectors. The cross-homology groups are completely determined by their dimensions, the *top* and *bottom* (k, l) -cross-Betti numbers $\beta_{k, l}^{(s)}(X) = \dim H_{k, l}^{(s)}(X)$, $s = 1, 2$. In particular, $\beta_{k-1}^{(1)}$ and $\beta_{-1, l}^{(2)}$ are the usual Betti numbers for the horizontal simplicial complexes [14]. The couple $\beta_{k, l} = (\beta_{k, l}^{(1)}, \beta_{k, l}^{(2)})$ is the (k, l) -cross-Betti vector of X and can be computed using basic Linear Algebra. These vectors are descriptors of the topologies of both the horizontal complexes and their inter-connections. For instance, $\beta_{0, -1}$ and $\beta_{-1, 0}$ encode the connectivities within and in-between the 1-skeletons of the horizontal complexes associated to X . Precisely, $\beta_{0, -1}^{(1)}$ is the number of connected components of the

graph $X_{1,-1}$ and $\beta_{0,-1}^{(2)}$ is the number of nodes in V_1 with no interconnections with any nodes in V_2 . Similarly, $\beta_{-1,0}^{(1)}$ is the number of nodes in V_2 with no interconnections with any nodes in V_1 , while $\beta_{-1,0}^{(2)}$ is the number of connected components of the bottom horizontal graph $X_{-1,1}$. Furthermore, $\beta_{1,-1}$ counts simultaneously the number of loops in $X_{1,-1}$ and the number of its intralayer links that do not belong to cross-triangles formed with the graph $X_{-1,1}$. Analogous topological information is provided by $\beta_{-1,1}$. Also, $\beta_{0,0}$ measures the extent to which individual nodes of one complex layer serve as communication channels between different hubs from the other layer. More precisely, an element in $H_{0,0}^{(1)}(X)$ represents either an interlayer 1-dimensional loop formed by a path in $X_{1,-1}$ whose end-nodes interconnect with the same node in V_2 , or two connected components in the top complex communicating with each other through a node in the bottom complex. In fact, $\beta_{0,0}$ counts the shortest paths of length 2 between nodes within one layer passing through a node from the other layer and not belonging to the cross-boundaries of cross-triangles; we call such paths *cones*. Put differently, $\beta_{0,0}$ quantifies node clusters in one layer that are "controlled" by nodes in the other layer. Detailed proof of this description is provided in Appendix A.

	$\mathcal{X}^{1,2}$	$\mathcal{X}^{1,3}$	$\mathcal{X}^{2,3}$
$\beta_{0,-1}^{\otimes}$	(1, 0)	(1, 0)	(1, 0)
$\beta_{1,-1}^{\otimes}$	(13, 21)	(13, 21)	(6, 14)
$\beta_{-1,0}^{\otimes}$	(0, 1)	(1, 1)	(0, 1)
$\beta_{-1,1}^{\otimes}$	(17, 6)	(29, 16)	(29, 16)
$\beta_{0,0}^{\otimes}$	(11, 14)	(20, 24)	(19, 23)

TABLE I: **Cross-Betti table.** The cross-Betti table for the CSM of Figure 1. The table quantifies the connectedness of the three horizontal complexes, the number of cycles in each of them, the number of nodes in each layer that are not connected to the other layers, the number of intra-layer edges not belonging to any cross-triangles, as well as the number of paths of length 2 connecting nodes in one layer and passing through a node from another layer.

Now, given a CSM \mathcal{X} , its *cross-Betti table* $\beta_{k,l}^{\otimes}$ is obtained by computing all the cross-Betti vectors of all its underlying CSB's. Computation of the cross-Betti table of the CSM of Fig. 1 is presented in Table I.

To illustrate what the cross-Betti vectors represent, we consider the simple 2-dimensional CSB X of Fig. 3. We get $\beta_{0,-1}^{(1)} = 2$, $\beta_{1,-1}^{(1)} = 1$, and $\beta_{-1,0}^{(2)} = 1$, $\beta_{-1,1}^{(2)} = 0$; which reflects the fact the top layer has 2 connected components and 1 cycle, while the bottom one has one component and no cycles. Moreover, 3 top nodes are not interconnected to the bottom complex, 6 top edges are not top faces of cross-triangles, 2 bottom nodes are not interconnect to the top layer, and 5 bottom edges are not bottom faces of cross-triangles. This information is encoded in $\beta_{0,-1} = (2, 3)$, $\beta_{1,-1} = (1, 6)$, $\beta_{-1,0} = (2, 1)$ and $\beta_{-1,1} = (5, 0)$. There are 3 generating interlayer cycles, two of which are formed by an intralayer path in the bottom layer and a node in the top layer (v_4^1 and v_6^1), and the other one is formed by an intralayer path in the top layer and a node (v_1^2) in the bottom layer. Moreover, the two nodes v_1^2 and v_4^2 of V_2 interconnect the two separated com-

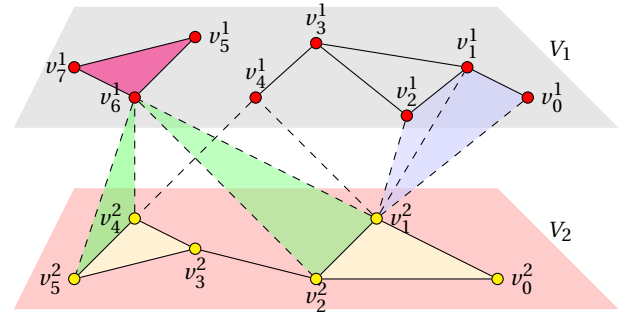


FIG. 3: **Cross-Betti vectors.** Schematic of a 2-dimensional CSB with 14 nodes in total, and whose oriented maximal crosssimplices are the intralayer triangle $[v_5^1, v_6^1, v_7^1]$ in $X_{2,-1}$, the intralayer edges $[v_0^1, v_1^1]$, $[v_1^1, v_2^1]$, $[v_1^1, v_3^1]$, $[v_2^1, v_3^1]$ in $X_{1,-1}$, the bottom intralayer triangles $[v_0^2, v_1^2, v_2^2]$, $[v_2^2, v_4^2, v_5^2]$ in $X_{-1,2}$, and the intralayer edge $[v_2^2, v_3^2]$ in $X_{-1,1}$, the cross-triangles $[v_0^1, v_1^1, v_1^2]$, $[v_1^1, v_2^1, v_1^2]$ in $X_{1,0}$, $[v_6^1, v_1^1, v_2^2]$, $[v_6^1, v_4^2, v_5^2]$ in $X_{0,1}$, and the cross-edges $[v_4^1, v_1^2]$, $[v_4^1, v_4^2]$ in $X_{0,0}$.

ponents of the top layer; they serve as *cross-hubs*: removing both nodes eliminates all communications between the two components of the top layer. Cross-hubs and these types of interlayer cycles are exactly what $\beta_{0,0}$ encodes. Specifically, by computing the cross-homology of X we get $\beta_{0,0}^{(1)} = 3$ which count the cycle $v_2^1 - v_3^1 - v_4^1 - v_1^1 - v_2^1$ and the nodes v_4^2 and v_1^2 that interconnect v_4^1 to v_6^1 and v_2^1 to v_6^1 , $\beta_{0,0}^{(2)} = 2$ counting the interlayer cycles $v_4^1 - v_1^1 - v_2^2 - v_3^2 - v_4^2 - v_1^1$ and $v_6^1 - v_2^1 - v_3^2 - v_4^2 - v_6^1$. In each of these cycles, the top node allows a shortest (interlayer) path between the end-points of the involved intralayer path.

Using algebraic-topological methods to calculate the cross-Betti vectors for larger multicomplexes can quickly become computationally heavy. We provide powerful linear-algebraic tools that not only allow to compute easily the $\beta_{k,l}$'s, but also tell exactly where the topological structures being counted are located within the multicomplex.

IV. SPECTRAL DESCRIPTORS

Cross-forms. Denote by $C^{k,l} := C^{k,l}(X, \mathbb{R})$ the dual space $\text{Hom}_{\mathbb{R}}(C_{k,l}, \mathbb{R})$ of the real vector space $C_{k,l}$. Namely, $C^{k,l}$ is the vector space of real linear functionals $\phi: C_{k,l} \rightarrow \mathbb{R}$. We will refer to such functionals as (k, l) -forms or *cross-forms* on X . In particular, $(k, -1)$ -forms correspond to k -forms on the simplicial complex $X_{\bullet,-1}$, and $(-1, l)$ -forms are l -forms on the complex $X_{-1,\bullet}$. We have $C^{-1,-1} = 0$, and by convention we set $C^{k,l}(\emptyset) = 0$.

Notice that a natural basis of $C^{k,l}$ is given by the set of linear forms

$$\{e_a: C_{k,l} \rightarrow \mathbb{R}, a \in X_{k,l}\},$$

called *elementary cross-forms*, where

$$e_a(b) = \begin{cases} 1, & \text{if } a = b, \\ 0, & \text{otherwise,} \end{cases}$$

which naturally identify $C^{k,l}$ with $C_{k,l}$. Now, define the maps $\delta_{k,l}^{(1)} : C^{k,l} \rightarrow C^{k+1,l}$ and $\delta_{k,l}^{(2)} : C^{k,l} \rightarrow C^{k,l+1}$ by the following equations

$$\begin{aligned}\delta_{k,l}^{(1)}\phi([a]) &= \sum_{b \in \partial^{(1)} a} \text{sgn}(b, \partial^{(1)} a) \phi([b]), \\ \delta_{k,l}^{(2)}\phi([c]) &= \sum_{d \in \partial^{(2)} c} \text{sgn}(d, \partial^{(2)} c) \phi([d]),\end{aligned}\quad (7)$$

for $\phi \in C^{k,l}$, $a \in X_{k+1,l}$ and $c \in X_{k,l+1}$. Next, given a weight w on X , we get an inner-product on cross-forms by setting

$$\langle \phi, \psi \rangle_{k,l} := \sum_{a \in X_{k,l}} w(a) \phi(a) \psi(a), \text{ for } \phi, \psi \in C^{k,l}. \quad (8)$$

It can be seen that, with respect to this inner-product, elementary cross-forms form an orthogonal basis, and by simple calculations, the dual maps are given by

$$(\delta_{k,l}^{(1)})^* \phi([a]) = \sum_{\substack{a' \in X_{k+1,l} \\ a \in \partial^{(1)} a'}} \frac{w(a')}{w(a)} \text{sgn}(a, \partial^{(1)} a') \phi([a']), \quad (9)$$

for $\phi \in C^{k+1,l}$, $a \in X_{k,l}$. And obviously we get a similar formula for the dual $(\delta_{k,l}^{(2)})^*$.

The cross-Laplacian operators. Identifying $C_{k,l}$ with $C^{k,l}$ and equipping it with an inner product as (8), we define the following self-adjoint linear operators on $C_{k,l}$ for all $k, l \geq -1$:

- the *top* (k, l) -cross-Laplacian

$$\mathcal{L}_{k,l}^{(T)} := (\delta_{k,l}^{(1)})^* \delta_{k,l}^{(1)} + \delta_{k-1,l}^{(1)} (\delta_{k-1,l}^{(1)})^*;$$

- and the *bottom* (k, l) -cross-Laplacian

$$\mathcal{L}_{k,l}^{(B)} := (\delta_{k,l}^{(2)})^* \delta_{k,l}^{(2)} + \delta_{k,l-1}^{(2)} (\delta_{k,l-1}^{(2)})^*.$$

Being defined on finite dimensional spaces, these operators can be represented as square matrices indexed over crosssimplices. Specifically, denoting $N_{k,l} = |X_{k,l}|$, $\mathcal{L}_{k,l}^{(T)}$ is represented by positive definite $N_{k,l} \times N_{k,l}$ -matrices (see Appendix B 2) for the general expressions).

Moreover, the null-spaces, the elements of which we call *harrmonic cross-forms*, are easily seen to be in one-to-one correspondence with cross-cycles on X . Namely, we have the following isomorphisms (see Appendix B 1 for the proof)

$$H_{k,l}^{(1)}(X) \cong \ker \mathcal{L}_{k,l}^{(T)}, \quad H_{k,l}^{(2)}(X) \cong \ker \mathcal{L}_{k,l}^{(B)}.$$

It follows that in order to compute the cross-Betti vectors, it suffices to determine the dimensions of the eigenspaces of the zero-eigenvalues of the cross-Laplacians.

It should be noted that in addition to being much easier to implement, the spectral method to compute cross-homology has the advantage of providing a geometric representation of the cross-Betti numbers through eigenvectors. But before we see how this works, let's make a few observations. Notice that $\mathcal{L}_{0,-1}^{(T)}$ and $\mathcal{L}_{-1,0}^{(B)}$ are the usual graph Laplacians of degree 0 for the horizontal complexes. And more generally, $\mathcal{L}_{k,-1}^{(T)}$ and $\mathcal{L}_{-1,l}^{(B)}$ are the combinatorial higher Hodge

ω_1	ω_2	ω_3	
0.0290	- 0.2872	0.2236	$[v_0^1; v_1^2]$
0.0290	- 0.2872	0.2236	$[v_1^1; v_1^2]$
0.0290	- 0.28721	0.2236	$[v_2^1; v_1^2]$
0.0	0.0	- 0.8944	$[v_4^1; v_1^2]$
0.7035	0.0710	0.0	$[v_4^1; v_4^2]$
- 0.0870	0.8616	0.2236	$[v_6^1; v_1^2]$
0.0	0.0	0.0	$[v_6^1; v_2^2]$
- 0.7035	- 0.0710	0.0	$[v_6^1; v_4^2]$
0.0	0.0	0.0	$[v_6^1; v_5^2]$

TABLE II: Harmonic $(0,0)$ -cross-forms. The 3 eigenvectors of the eigenvalue 0 of $\mathcal{L}_{0,0}^{(T)}$ corresponding to the synthetic CSB of Figure 3. There are 2 harmonic cross-hubs: v_1^2 and v_4^2 , their respective harmonic cross-hubness are 2.6177 and 1.4070.

Laplacians [15, 19, 31] of degree k and l , respectively, for the horizontal simplicial complexes. Furthermore, $\mathcal{L}_{k,-1}^{(B)}$ (resp. $\mathcal{L}_{-1,l}^{(T)}$) detects the k -simplices (resp. l -simplices) in the top (resp. bottom) layer complex that are not top (resp. bottom) faces of $(k,0)$ -crosssimplices (resp. $(0,l)$ -crosssimplices). Moreover, one can see that $\mathcal{L}_{k,-1}^{(B)}$ is the diagonal matrix indexed over the k -simplices on the top complex and whose diagonal entries are the BO degrees. Similarly, $\mathcal{L}_{-1,l}^{(T)}$ is the diagonal matrix whose diagonal entries are the TO degrees of the l -simplices on the bottom complex. This is consistent with the interpretation of the cross-Betti numbers $\beta_{0,-1}^{(2)}$ and $\beta_{-1,0}^{(1)}$ given earlier in terms of connectivities between the 1-skeletons of the horizontal complexes.

Harmonic cross-hubs. Assume for the sake of simplicity that the X is equipped with the trivial weight $\cong 1$. Then, by (B4), the $(0,0)$ -cross-Laplacians $\mathcal{L}_{0,0}^{(T)}$ and $\mathcal{L}_{0,0}^{(B)}$ are respectively represented by the $N_{0,0} \times N_{0,0}$ -matrices indexed on cross-edges $a_i, a_j \in X_{0,0}$ whose entries are given by

$$(\mathcal{L}_{0,0}^{(T)})_{a_i, a_j} = \begin{cases} \deg_{TO}(a_i) + 1, & \text{if } i = j, \\ 1, & \text{if } i \neq j, [a_i] = [v_i^1; v_k^2], \\ & [a_j] = [v_j^1; v_k^2] \\ & \text{and } \{v_i^1, v_j^1, v_k^2\} \notin X_{1,0}, \\ 0, & \text{otherwise,} \end{cases} \quad (10)$$

and

$$(\mathcal{L}_{0,0}^{(B)})_{a_i, a_j} = \begin{cases} \deg_{BO}(a_i) + 1, & \text{if } i = j, \\ 1, & \text{if } [a_i] = [v_{i_0}^1; v_i^2], \\ & [a_j] = [v_{i_0}^1; v_j^2], \\ & \text{and } \{v_{i_0}^1, v_i^2, v_j^2\} \notin X_{0,1}, \\ 0, & \text{otherwise.} \end{cases} \quad (11)$$

Applied to the toy example of Fig. 3, $\mathcal{L}_{0,0}^{(T)}$ has a zero-eigenvalue of multiplicity 3, generating the three $(0,0)$ -cross-cycles in Table II.

Each coordinate in the eigenvectors is seen as an "intensity" along the corresponding cross-edge. Cross-edges with non-zero intensities sharing the same bottom node define certain communities in the top complex that are "controlled" by the involved bottom node. These community structures depend on both the underlying topology of the top complex and its interdependence with the other complex layer.

We then refer to them as *harmonic cross-clusters*, and the bottom nodes controlling them are thought of as *harmonic cross-hubs* (HCH). The *harmonic cross-hubness* of a bottom node is the L^1 -norm of the intensities of all cross-edges having it in common. Here, in the eigenvectors of the eigenvalue 0, there are two subsets of cross-edges with non-zero coordinates: the cross-edges with v_1^2 in common, and the ones with v_4^2 in common. We therefore have two harmonic cross-hubs (see illustration in Fig. 5), hence two harmonic cross-clusters. The first one is responsible for the top layer cross-cluster $\{v_0^1, v_1^1, v_2^1, v_4^1, v_6^1\}$, while the second one controls the top layer cross-cluster $\{v_4^1, v_6^1\}$. The intensity of each involved cross-edge is the L^1 -norm of its corresponding coordinates in the 3 eigenvectors, and the harmonic cross-hubness is the sum of the intensities of the cross-edges interconnecting the corresponding cross-hub to each of the top nodes in the cross-clusters it controls. For instance, v_1^2 is the bottom node with the highest harmonic cross-hubness which is 2.6177. This reflects the fact v_1^2 not only interconnects the two connected components of the top complex (which v_4^2 does as well), but it also allows fast-track connections between the highest number of nodes that are not directly connected with intra-layer edges in the top complex. The same calculations applied to the eigenvectors of the zero-eigenvalues of $\mathcal{L}_{0,0}^{(B)}$ give v_6^1 as the top node with the highest harmonic cross-hubness w.r.t. the bottom complex.

Spectral persistence of cross-hubs. To better grasp the idea of cross-hubness, let us have a closer look at the coordinates of the eigenvectors of the $(0, 0)$ -cross-Laplacians ((10) and (11)) whose eigenvalues are all non-negative real numbers. Suppose $\phi = (x_1, \dots, x_{N_{0,0}})$ is an eigenvector for an eigenvalue λ^T of $\mathcal{L}_{0,0}^{(T)}$. Then, denoting the cross-edges by $a_i, i = 1, \dots, N_{0,0}$, we have the relations

$$x_i = \frac{1}{\lambda^T - \deg_{TO}(a_i)} \sum_j \chi(a_i, a_j) x_j, \quad (12)$$

where χ is such that $\chi(a_i, a_j) = 1$ if $i = j$ or if a_i and a_j are adjacent but do not belong to a top cross-triangle, and $\chi(a_i, a_j) = 0$ otherwise. It follows that the cross-edge intensity $|x_i|$ grows larger as $\deg_{TO}(a_i) \rightarrow \lambda^T$. In particular, for $\lambda^T = 0$, the intensity is larger for cross-edges that belong to a large number of cones and to the smallest number of top cross-triangles. Now, consider the other extreme of the spectrum, namely $\lambda^T = \lambda_{max}^T$ to be the largest eigenvalue of $\mathcal{L}_{0,0}^{(T)}$. Then, the intensity $|x_i|$ is larger for cross-edges belonging to the largest number of top cross-triangles and a large number of top cones at the same time.

Taking the case of a 2-layered network, for $\lambda^T = 0$, $|x_i|$ is larger for a cross-edge pointing to a bottom node interconnecting a largest number of top nodes that are not directly connected with intra-layer edges; and for $\lambda^T = \lambda_{max}$, $|x_i|$ is larger for a cross-edge pointing to a bottom node interconnecting a large number of top intra-layer communities both with each other and with a large number of top nodes that are not directly connected to each other via intra-layer edges.

More generally, by applying the same process to each distinct eigenvalue, we obtain clustering structures in the top

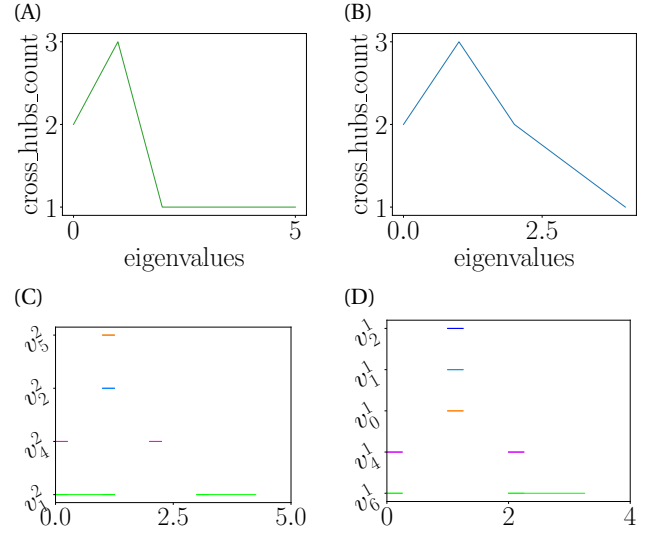


FIG. 4: Spectral persistence of cross-hubs. Schematic illustrations of the variations of spectral cross-hubs along the eigenvalues and the spectral persistence bar codes for the toy CSB of Fig. 3: (A) shows the number of bottom nodes that emerge as spectral cross-hubs w.r.t. the top layer as a function of the eigenvalues of $\mathcal{L}_{0,0}^{(T)}$, and (B) represents the number of top nodes revealed as spectral cross-hubs w.r.t. the bottom layer as a function of the eigenvalues of $\mathcal{L}_{0,0}^{(B)}$. (C) and (D) represent the *spectral persistence bar codes* for $\mathcal{L}_{0,0}^{(T)}$ and $\mathcal{L}_{0,0}^{(B)}$, respectively. For both the top and bottom $(0, 0)$ -cross-Laplacians, most of the spectral cross-hubs, hence of spectral cross-clusters, emerge during the first stages (smallest eigenvalues), very few of them survive at later stages, and here only one cross-hub emerge or survive at the largest eigenvalue (v_1^2 for $\mathcal{L}_{0,0}^{(T)}$ and v_6^1 for $\mathcal{L}_{0,0}^{(B)}$).

layer that are *controlled* by the bottom nodes and that vary along the spectrum $\lambda_1^T \leq \lambda_2^T \leq \dots \leq \lambda_{max}^T$ of $\mathcal{L}_{0,0}^{(T)}$. At every stage, we regroup the cross-edges with non-zero coordinates in the associated eigenvectors and pointing to the same nodes, then sum up their respective intensities to obtain a ranking among a number of cross-hubs that we call *spectral cross-hubs* (SCHs). Intuitively, the intensities held by cross-edges gather to confer a 'restructuring power' onto the common bottom node – the cross-hub, allowing it to control a cluster on the top layer. It is clear that, by permuting the top layer with the bottom layer, the same reasoning applies to $\mathcal{L}_{0,0}^{(B)}$. In particular, we define the *principal cross-hubs* (PCH) in the bottom layer w.r.t. the top layer as the SCHs obtained from λ_{max}^T . The *principal cross-hubness* of a bottom PCH is defined as its restructuring power. In a similar fashion, we define the principal cross-hubness in the top layer w.r.t. the bottom layer using the largest eigenvalue λ_{max}^B of $\mathcal{L}_{0,0}^{(B)}$. Going back to the bicomplex of Fig. 3, the largest eigenvalue of $\mathcal{L}_{0,0}^{(T)}$ is $\lambda_{max}^T = 5$, the corresponding eigenvector is represented by Table III.

There is only one PCH in the bottom layer w.r.t. the top layer, which is the bottom node v_1^2 , and its principal cross-hubness is 2.2360.

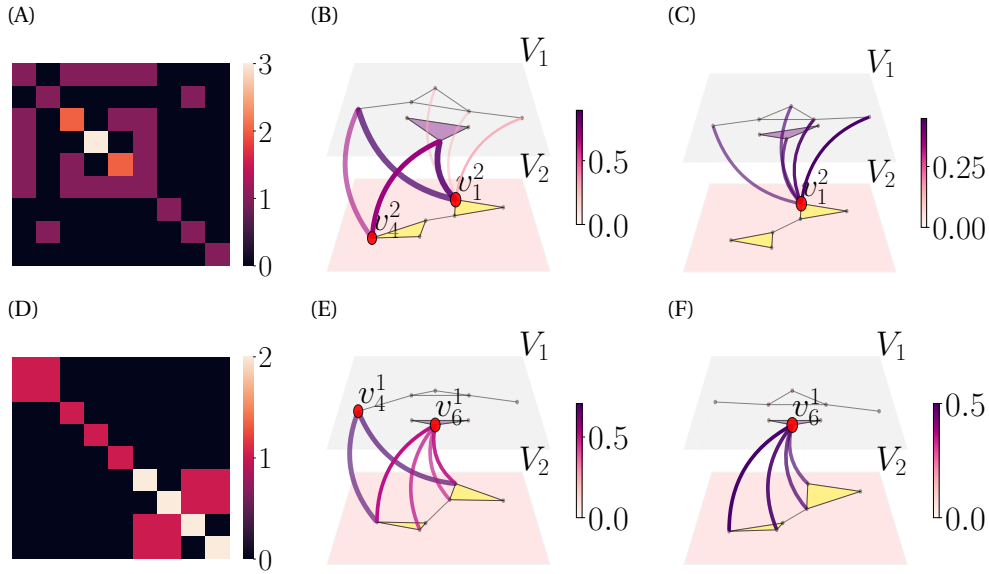


FIG. 5: **Cross-Laplacians, harmonic and principal cross-hubs.** (A) and (D): Heat-maps of the the top and bottom $(0,0)$ -cross-Laplacian matrices for the example of Fig. 3. Both matrices are indexed over the cross-edges of the CSB, and the diagonal entries correspond to one added to the number of cross-triangles containing the corresponding cross-edge. $\mathcal{L}_{0,0}^{(T)}$ has a zero eigenvalue of multiplicity 3, while $\mathcal{L}_{0,0}^{(B)}$ has a zero eigenvalue of multiplicity 2. (B) and (E): The harmonic cross-hubs w.r.t. to the top (resp. the bottom) horizontal complex of X ; the *intensity* of a cross-edge is given by the L^1 -norm of the corresponding coordinates in the eigenvectors of the eigenvalue 0. (C) and (F): the *principal cross-hubs* in the bottom (resp. top) layer w.r.t. the top (resp. bottom) layer; by definition, they are the spectral cross-hubs obtained from by the largest eigenvalues of the top and bottom $(0,0)$ -cross-Laplacians, respectively.

0.4472	$[v_0^1; v_1^2]$
0.4472	$[v_1^1; v_1^2]$
0.4472	$[v_2^1; v_1^2]$
0.4472	$[v_4^1; v_1^2]$
0.0	$[v_4^1; v_4^2]$
0.4472	$[v_6^1; v_2^2]$
0.0	$[v_6^1; v_5^2]$
0.0	$[v_6^1; v_4^2]$
0.0	$[v_6^1; v_5^2]$

TABLE III: Principal eigenvector of $\mathcal{L}_{0,0}^{(T)}$ for the CSB of Figure 3. By definition, this is the eigenvector associated to the largest eigenvalue.

Interestingly, the number of SCHs that appear for a given eigenvalue tend to vary dramatically w.r.t. the smallest eigenvalues before it eventually decreases or stabilizes at a very low number (see Fig. 4 and Fig. 6). Some cross-hubs may appear at one stage along the spectrum and then disappear at a future stage. This suggests the notion of *spectral persistence* of cross-hubs. Nodes that emerge the most often or live longer as cross-hubs along the spectrum might be seen as the most central in restructuring the topology of the other complex layer. The more we move far away from the smallest non-zero eigenvalue, the most powerful are the nodes that emerge as hubs facilitating communications between aggregations of nodes in the other layer. The emergence of spectral cross-hubs is represented by a horizontal line - *spectral persistence bar* - running through the indices of the

corresponding eigenvalues (Fig. 4). The spectral persistence bars corresponding to all SCHs (the *spectral bar codes*) obtained from $\mathcal{L}_{0,0}^{(T)}$ (resp. $\mathcal{L}_{0,0}^{(B)}$) constitute a *signature* for all the clustering structures imposed by the bottom (resp. top) layer to the top (resp. bottom) layer.

V. EXPERIMENTS ON MULTIPLEX NETWORKS

Diffusion CSBs. Let \mathcal{M} be a multiplex formed by M graphs $\Gamma^s = (E_s, V)$, $s = 1, \dots, M$. Denoting the vertex set V as an ordered set $\{1, 2, \dots, N\}$, we will write v_i^s to represent the node i in the graph Γ^s , following the same notations we have used for multicomplexes.

For every pair of distinct indices s, t , we define the 2-dimensional CSB $X^{s \rightarrow t}$ on $V \times V$ such that $X_{k,-1}^{s \rightarrow t} = \emptyset$ for $k \geq 1$, $X_{-1,k}^{s \rightarrow t}$ is the 2-clique complex of the layer indexed by t in the multiplex \mathcal{M} ; a pair $(v_i^s, v_j^t) \in V \times V$, forms a cross-edge if $i < j$, and nodes i and j are connected in Γ^s ; and a $(0,1)$ -crosssimplex is a triple $(v_i^s, v_j^t, v_k^t) \in V^3$ such that i is connected to j and k in Γ^s , and j and k are connected in Γ^t , while $X_{1,0}^{s \rightarrow t} = \emptyset$. We call $X^{s \rightarrow t}$ the *diffusion bicomplex* of (layer) s onto t . Notice that by construction, the $(0,0)$ -cross-Laplacians of $X^{s \rightarrow t}$ are indexed over E_s , while the $(0,0)$ -cross-Laplacians of $X^{t \rightarrow s}$ are indexed over E_t . This shows that $X^{s \rightarrow t}$ and $X^{t \rightarrow s}$ are not the same. In fact, the diffusion bicomplex $X^{s \rightarrow t}$ is a way to look at the topology of Γ^s through the topology of Γ^t ; or put differently, it diffuses

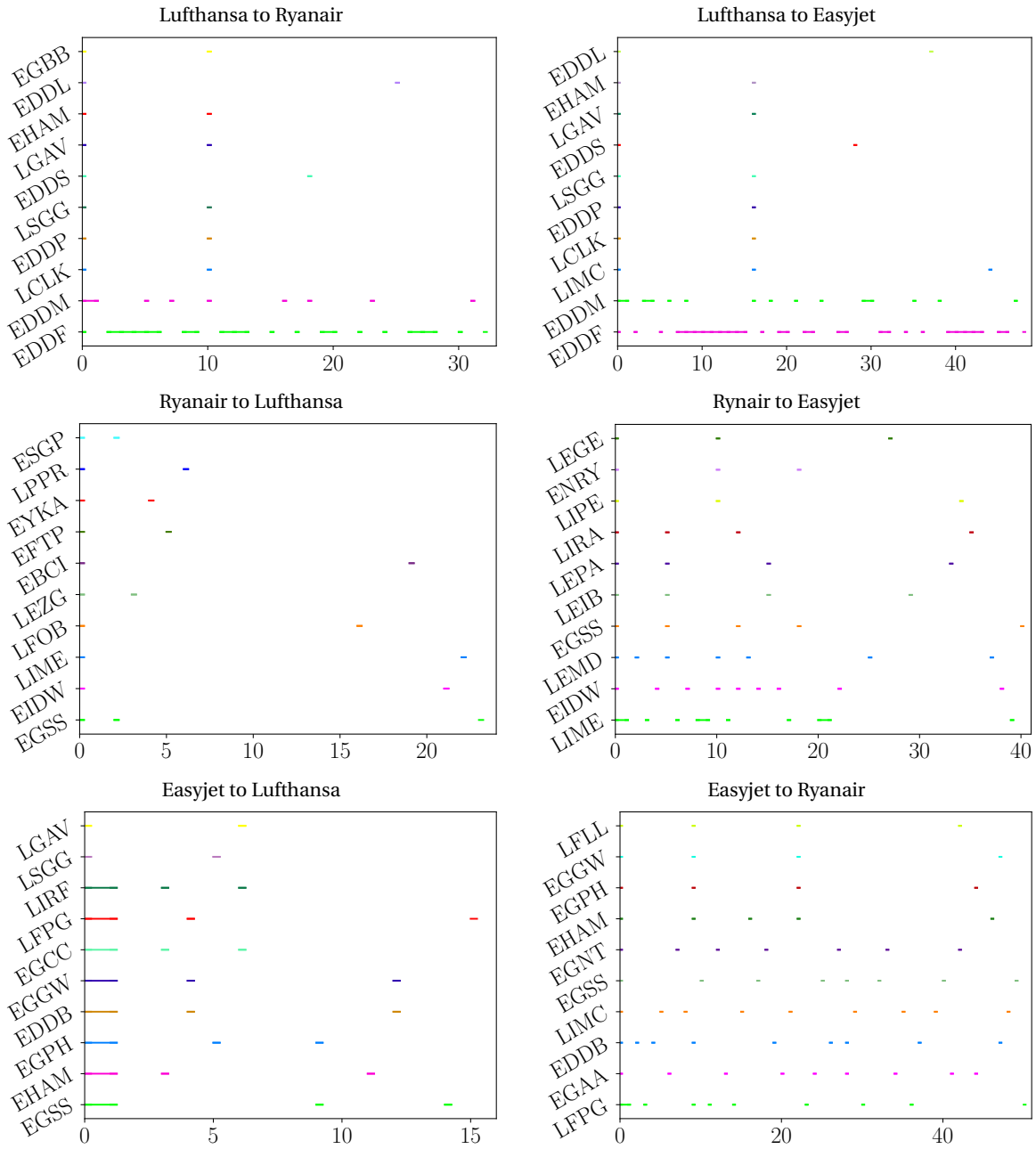


FIG. 6: **Spectral persistent cross-hubs.** The spectral persistence bar codes of the six diffusion bicomplexes of the European ATN multiplex. The nodes represent European airports labelled with their ICAO codes. The most persistent cross-hubs correspond to the airports that provide the most efficient correspondences from the first airline network to the second.

the topology of the former into the topology of the latter.

Cross-hubs in air transportation networks. We use a subset of the European Air Transportation Network (ATN) dataset from [5] to construct a 3-layered multiplex \mathcal{M} on 450 nodes each representing a European airport [36]. The 3 layer networks Γ^1 , Γ^2 , and Γ^3 of \mathcal{M} represent the direct flights served by Lufthansa, Ryanair, and Easyjet airlines, respectively; that is, intra-layer edges correspond to direct flights between airports served by the corresponding airline. Considering the respective bottom $(0, 0)$ -cross-Laplacians of the

six diffusion bicomplexes $X^{1 \rightarrow 2}$, $X^{1 \rightarrow 3}$, $X^{2 \rightarrow 1}$, $X^{3 \rightarrow 1}$, $X^{2 \rightarrow 3}$, and $X^{3 \rightarrow 2}$, we obtain the spectral persistence bar codes describing the emergence of SCH's for each airline w.r.t. the others (see Fig. 6). The induced SCH rankings are presented in Table V, while the corresponding PCHs are illustrated in Fig. 7.

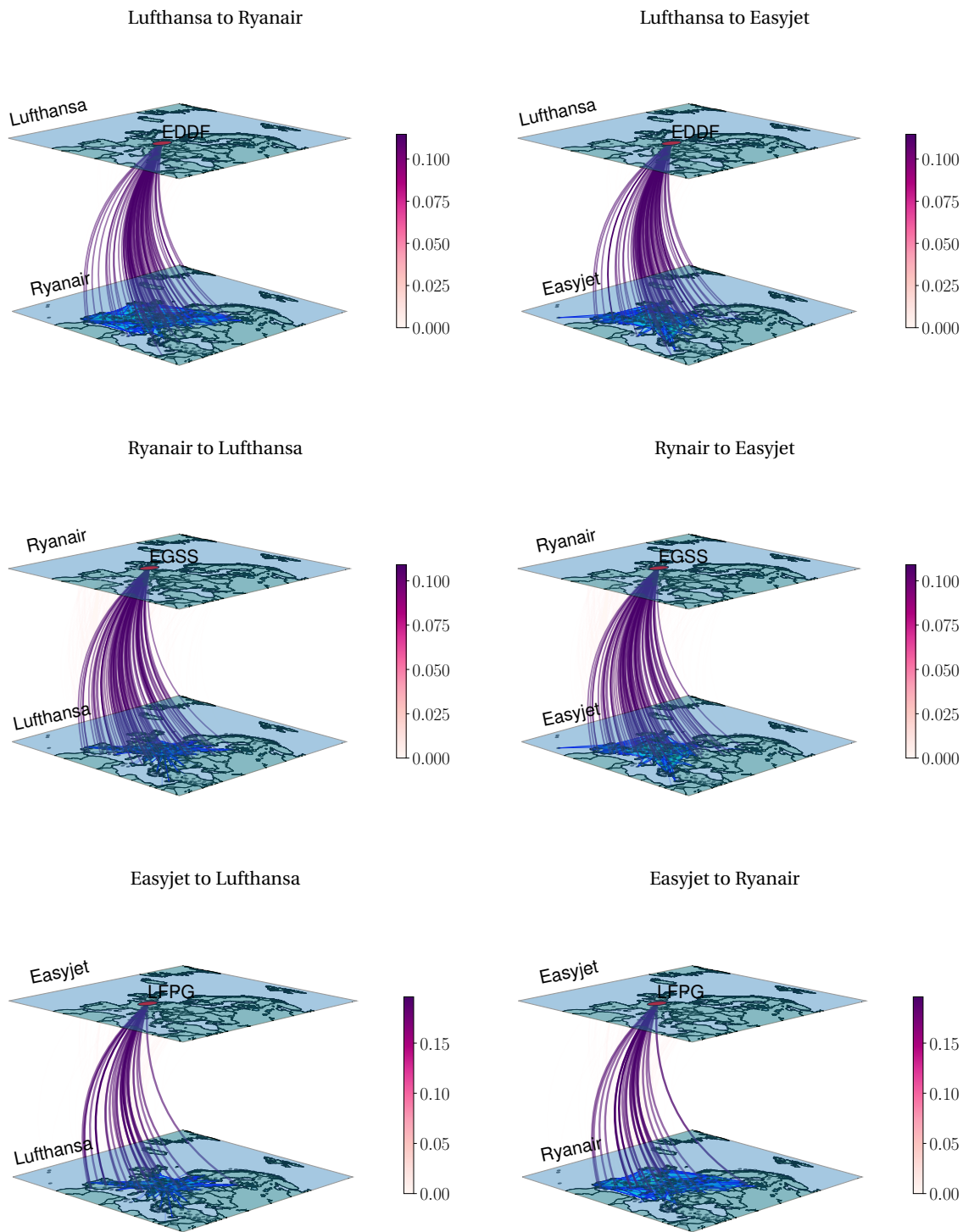


FIG. 7: PCHs of the diffusion bicomplexes for the European ATN multiplex. The nodes represent airports labelled with their ICAO codes.

VI. DISCUSSION AND CONCLUSIONS

We have introduced CSM as a generalization of both the notions of simplicial complexes and multilayer networks. We

further introduced cross-homology to study their topology and defined the cross-Laplacian operators to detect more structures that are not detected by homology. Our goal here was to set up a mathematical foundation for studying higher-

1. $X^{Lufthansa \rightarrow Ryanair}$		2. $X^{Lufthansa \rightarrow Easyjet}$	
Airports	Rank	Airports	Rank
Frankfurt Airport	1	Frankfurt Airport	1
Munich Airport	2	Munich Airport	2
Düsseldorf Airport	3	Milan Malpensa Airport	3
Stuttgart Airport	4	Düsseldorf Airport	4
Larnaca Airport	5	Stuttgart Airport	5
Leipzig Halle Airport	5	Larnaca Airport	6
Geneva Airport	5	Leipzig Halle Airport	6
Athens Airport	5	Geneva Airport	6
Amsterdam Airport Schiphol	5	Athens Airport	6
Birmingham Airport	5	Amsterdam Airport Schiphol	6
		Birmingham Airport	6

3. $X^{Ryanair \rightarrow Lufthansa}$		4. $X^{Ryanair \rightarrow Easyjet}$	
Airports	Rank	Airports	Rank
London Stansted Airport	1	Bergamo Airport	1
Bergamo Airport	2	Dublin Airport	2
Dublin Airport	3	London Stansted Airport	3
Charleroi Airport	4	Madrid Barajas Airport	4
Paris Beauvais Airport	5	Rome Ciampino Airport	5
Porto Airport	6	Palma de Mallorca Airport	6
Tampere Airport	7	Ibiza Airport	7
Kaunas Airport	8	Bologna Airport	8
Zaragoza Airport	9	Girona Airport	9
Göteborg City Airport	10	Moss Airport Rygge	10

5. $X^{Easyjet \rightarrow Lufthansa}$		6. $X^{Easyjet \rightarrow Ryanair}$	
Airports	Rank	Airports	Rank
Paris Charles de Gaulle Airport	1	Paris Charles de Gaulle Airport	1
London Stansted Airport	2	London Stansted Airport	2
Berlin Brandenburg Airport	3	Milan Malpensa Airport	3
London Luton Airport	4	Berlin Brandenburg Airport	4
Amsterdam Airport Schiphol	5	Belfast International Airport	5
Edinburgh Airport	6	London Luton Airport	6
Manchester Airport	7	Amsterdam Airport Schiphol	7
Rome Fiumicino Airport	8	Edinburgh Airport	8
Athens Airport	9	Newcastle Airport	9
Geneva Airport	10	Lyon-Saint Exupéry Airport	10

TABLE IV: Ranking of the ten most persistent SCHs for the diffusion bicomplexes associated to the European air transportation multiplex network.

order multilayer complex systems. Nevertheless, through synthetic examples of CSM and applications to multiplex networks, we have shown that our framework provides powerful tools to revealing important topological features in a multilayer networks and address questions that would not arise from the standard pairwise-based formalism of multilayer networks. We put a special focus on the $(0,0)$ -cross-Laplacians to show how their spectra quantify the extent to which nodes in one layer restructure the topology of other layers in a multilayer network. Indeed, given a CSB X or even a 2-layered network, we defined $\mathcal{L}_{0,0}^{(T)}$ and $\mathcal{L}_{0,0}^{(B)}$ as two self-adjoint positive operators operators that allow to look at the topology of one layer through the lens of the other layer. Specifically, we saw that their spectra allow to detect nodes from one layer that serve as interlayer connecting hubs for clusters in the other layer; we referred to such nodes as spectral cross-hubs (SCHs). Such hubs vary in function of the eigenvalues of the cross-Laplacians, the notion of *spectral*

persistent cross-hubs was used to rank them according to their frequency along the spectra. The SCHs obtained from the largest eigenvalues were referred here as *principal cross-hubs* (PCHs) as they are the ones that interconnects the most important structures of the other layer. We should note that a PCH is not necessarily spectrally persistent, and two SCHs can be equally persistent but at different ranges of the spectrum. This means that, depending on the applications, some choices need to be made when ranking SCHs based on their spectral persistence. Indeed, it might be the case that two SCHs persist equally longer enough to be considered as the most persistent ones, but that one persists through the first quarter of the spectrum while the other persists through the second quarter of the spectrum, so that none of them is a PCH. For instance, in the example of the European ATN multiplex networks, when two nodes were equally persistent, we ranked higher the one that came later along the spectrum. Finally, one can observe that the topological and geometric

interpretations given for these operators can be generalized to the higher-order (k, l) -cross-Laplacians as well. That is, the spectra of these operators encode the extent to which higher-order topological structures (edges, triangles, tetrahedrons, and so on) control the emergence of higher-order clustering structures in the other layers.

Acknowledgments

This work was supported by the Natural Sciences and Engineering Research Council of Canada through the CRC grant NC0981.

Appendix A: Description of the $(0, 0)$ -cross-Betti vectors

Cones and kites. Let v_j^2 be a fixed vertex in V_2 . A *kite from V_1 to v_j^2* is an ordered tuple $(v_{i_1}^1, \dots, v_{i_p}^1)$ of vertices in V_1 such that $\{v_{i_r}^1, v_{i_{r+1}}^1, v_j^2\} \in X_{1,0}$ for $r = 1, \dots, p-1$. Such an object is denoted as $(v_{i_0}^1, \dots, v_{i_p}^1 \leftarrow v_j^2)$. Beware that the vertices $v_{i_1}^1, \dots, v_{i_p}^1$ do not need to be pair-wise connected in V_1 . What we have here are cross-triangles all pointing to v_j^2 that are pieced together in the form of an actual kite as in Figure 8. In particular, if v_j^2 is the bottom face of a $(1, 0)$ -cross-triangle $[v_i^1, v_k^1; v_j^2]$, then $(v_i^1, v_k^1 \leftarrow v_j^2)$ is a kite. If $(v_{i_1}^1, \dots, v_{i_p}^1 \leftarrow v_j^2)$ is a kite, its *boundary* is the triple $(v_{i_1}^1, v_{i_p}^1, v_j^2) \in V_1^2 \times V_2$. Similarly, given a fixed vertex $v_i^1 \in V_1$, one can define a *kite from V_2 to v_i^1* by a tuple $(v_{j_1}^2, \dots, v_{j_{p'}}^2)$ of vertices in V_2 satisfying analogous conditions. Such a kite will be denoted as $(v_i^1 \rightarrow v_{j_1}^2, \dots, v_{j_{p'}}^2)$.

It is worth noting that if $(v_{i_1}^1, \dots, v_{i_p}^1)$ is a kite from V_1 to v_j^2 , then so is each tuple $(v_{i_r}^1, v_{i_{r+1}}^1, \dots, v_{i_{r+q}}^1)$ with $1 \leq r$ and $r+q \leq p$.

By a *cross-chain* on a kite we mean one that is a linear combination of the triangles composing the kite; that is, a cross-chain on the kite $(v_{i_1}^1, \dots, v_{i_p}^1 \leftarrow v_j^2)$ is an element $a \in C_{1,0}(X)$ of the form

$$a = \sum_{r=1}^{p-1} \gamma_r [v_{i_r}^1, v_{i_{r+1}}^1; v_j^2], \quad (\text{A1})$$

where $\gamma_1, \dots, \gamma_{p-1} \in \mathbb{R}$. In a similar fashion, cross-chains on a kite of the form $(v_i^1 \rightarrow v_{j_1}^2, \dots, v_{j_{p'}}^2)$ are defined.

Now, given a pair (v_i^1, v_k^1) of vertices in the layer V_1 and the vertex $v_j^2 \in V_2$, we say that the triple $(v_i^1, v_k^1, v_j^2) \in V_1^2 \times V_2$ is a *cone with base (v_i^1, v_k^1) and vertex v_j^2* if it satisfies the following conditions:

- $v_i^1 \sim v_j^2$ and $v_k^1 \sim v_j^2$; i.e., $[v_i^1; v_j^2], [v_k^1; v_j^2] \in X_{0,0}$;
- the triple $(v_i^1, v_k^1, v_j^2) \in V_1^2 \times V_2$ is not the boundary of a kite from V_1 to v_j^2 .

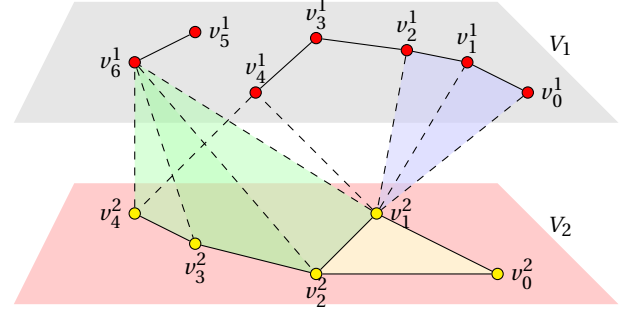


FIG. 8: A 2-dimensional crosssimplicial bicomplex containing kites and cones. Indeed (v_0^1, v_1^1, v_2^1) is kite from V_1 to $v_1^2 \in V_2$ with boundary $(v_0^1, v_1^1, v_2^1) \in V_1^2 \times V_2$ and $(v_2^1, v_2^2, v_3^2, v_4^2)$ is a kite from V_2 to $v_1^2 \in V_1$ with boundary $(v_2^1, v_2^2, v_3^2, v_4^2) \in V_1 \times V_2^2$. The tuples (v_2^1, v_2^2, v_3^2) , (v_2^1, v_2^2) , and (v_2^2, v_3^2, v_4^2) are also kites from V_2 to v_1^2 . Furthermore, there are 3 cones with bases in V_1 : (v_2^1, v_4^1, v_1^2) is a closed cone with base $(v_2^1, v_4^1) \in V_1$ and vertex $v_1^2 \in V_2$, and (v_4^1, v_6^1, v_1^2) is an open cone with base $(v_4^1, v_6^1) \in V_1^2$ and vertex $v_1^2 \in V_2$. Also, (v_4^1, v_6^1, v_4^2) is an open cone with base $(v_4^1, v_6^1) \in V_1^2$ and vertex $v_4^2 \in V_2$; and $(v_1^2, v_4^2, v_4^1) \in V_2^2 \times V_1$ is a closed cone with base $(v_1^2, v_4^2) \in V_2^2$ and vertex $v_4^1 \in V_1$. It follows from Theorem A.1 that $\beta_{0,0} = (3, 1)$.

We also say that (v_i^1, v_k^1, v_j^2) is a *cone with base in V_1 and vertex in V_2* . In a similar fashion one defines a cone with base in V_2 and vertex in V_1 . We refer to Figure 8 for examples of cones.

An immediate consequence of a triple $(v_i^1, v_k^1, v_j^2) \in V_1^2 \times V_2$ being a cone is that the vertices $\{v_i^1, v_k^1, v_j^2\}$ is not a $(1, 0)$ -crosssimplex. The vertices v_i^1 and v_k^1 might however be connected by a *horizontal path* of some length; by which we mean that there might be a sequence of vertices $v_{i_0}^1, \dots, v_{i_p}^1$ in V_1 not all of which form cross-triangles with v_j^2 and such that

$$v_i^1 \frown^{(1)} v_{i_0}^1 \frown^{(1)} \dots \frown^{(1)} v_{i_p}^1 \frown^{(1)} v_k^1,$$

in which case the cone is said to be *closed*; it is called *open* otherwise.

Cones in a crosssimplicial bicomplex are classified by the top and bottom $(0, 0)$ -cross-homology groups of the bicomplex. Specifically, we have the following topological interpretation of $H_{0,0}^{(1)}(X)$, $H_{0,0}^{(2)}(X)$, and hence, the $(0, 0)$ -cross-Betti numbers.

Theorem A.1. *The $(0, 0)$ -cross-homology group $H_{0,0}^{(1)}(X)$ (resp. $H_{0,0}^{(2)}(X)$) is generated by the cross-homology classes of cones with bases in V_1 and vertices in V_2 (resp. with bases in V_2 and vertices in V_1). Therefore, the $(0, 0)$ -cross-Betti number $\beta_{0,0}^{(t)}$ counts the generating cones with bases in V_t , $t = 1, 2$.*

Here, by the cross-homology class of the cone $(v_i^1, v_k^1, v_j^2) \in V_1^2 \times V_2$, for instance, we mean the top cross-homology of the $(0, 0)$ -cross-chain $[v_k^1; v_j^2] - [v_i^1; v_j^2] \in C_{0,0}(X)$.

Proof. We prove the theorem for $H_{0,0}^{(1)}(X)$ since the same arguments apply to $H_{0,0}^{(2)}(X)$. Every cone (v_i^1, v_k^1, v_j^2) defines a non-trivial $(0,0)$ -cross-cycle; namely, the difference of the corresponding cross-edges $[v_i^1; v_j^2] - [v_k^1; v_j^2] \in \ker \partial_{0,0}^{(1)}$. More generally, suppose we are given p cones $(v_{i_1}^1, v_{i_2}^1, v_j^2), (v_{i_2}^1, v_{i_3}^1, v_j^2), \dots, (v_{i_{p-1}}^1, v_{i_p}^1, v_j^2)$ with bases in V_1 and all with the same vertex $v_j^2 \in V_2$. Then, for all real numbers $\alpha_1, \dots, \alpha_p$ such that $\sum_{r=1}^p \alpha_r = 0$, the cross-chain

$$b = \sum_{r=1}^p \alpha_r [v_{i_r}^1; v_j^2] \quad (\text{A2})$$

is clearly a $(0,0)$ -cross-cycle with non-trivial cross-homology class; i.e., $b \in \ker \partial_{0,0}^{(1)}$ and $b \notin \text{im} \partial_{1,0}^{(1)}$. Conversely, let $b' \in \ker \partial_{0,0}^{(1)}$. We can write

$$b' = \sum_{m=1}^M \alpha'_m [v_{i_m}^1; v_{i_m}^2] \in C_{0,0}(X),$$

so that $\partial_{0,0}^{(1)}(b') = \sum_{m=1}^M \alpha'_m [v_{i_m}^2] = 0$. Then, either all the $v_{i_m}^2$'s are pair-wise different, in which case b' is the trivial cross-cycle; or there exist $p+1$ subsets $(\{m_{r,1}, \dots, m_{r,M_r}\})_{r=1}^{p+1}$ of $\{1, \dots, M\}$ such that

$$v_{i_{m_{r,1}}}^2 = v_{i_{m_{r,2}}}^2 = \dots = v_{i_{m_{r,M_r}}}^2, \text{ for } 1 \leq r \leq p,$$

and

$$v_{i_{m_{p+1,j}}}^2 \neq v_{i_{m_{p+1,j'}}}^2, \text{ for all } j \neq j', 1 \leq j, j' \leq M_{p+1}.$$

It follows that

$$\sum_{j=1}^{M_r} \alpha'_{m_{r,j}} = 0, \text{ for each } r = 1, \dots, p, \quad (\text{A3})$$

and $\alpha'_{m_{p+1,j}} = 0$ for all $j = 1, \dots, M_{p+1}$. Hence, we get the following general expression of a $(0,0)$ -cross-cycle:

$$b' = \sum_{r=1}^p \sum_{j=1}^{M_r} \alpha'_{m_{r,j}} [v_{i_{m_{r,j}}}^1; v_{i_{m_{r,1}}}^2], \quad (\text{A4})$$

where the coefficients satisfy (A3). Furthermore, it is straightforward to see that $b' \in \text{im} \partial_{1,0}^{(1)}$ if and only if for each $r = 1, \dots, p$, there exists a permutation τ_r of $\{1, \dots, M_r\}$ such that

$$(v_{i_{m_{r,\tau_r(1)}}}^1, \dots, v_{i_{m_{r,\tau_r(M_r)}}}^1 \leftarrow v_{i_{m_{r,1}}}^2)$$

is a kite. In that case, we get $b' = \partial_{1,0}^{(1)}(a)$ where

$$a = \sum_{r=1}^p \sum_{r=1}^{M_r-1} \gamma_{m_{r,j}} [v_{i_{m_{r,\tau_r(j)}}}^1, v_{i_{m_{r,\tau_r(j+1)}}}^1; v_{i_{m_{r,1}}}^2], \quad (\text{A5})$$

and where for $r = 1, \dots, p$, the coefficients $\gamma_{m_{r,j}}$ are given by

$$\begin{cases} \gamma_{m_{r,1}} &= -\alpha'_{m_{r,\tau_r(1)}} \\ \gamma_{m_{r,2}} &= -\alpha'_{m_{r,\tau_r(1)}} - \alpha'_{m_{r,\tau_r(2)}} \\ &\vdots \\ \gamma_{m_{r,M_r-2}} &= -\alpha'_{m_{r,\tau_r(1)}} - \alpha'_{m_{r,\tau_r(2)}} - \dots - \alpha'_{m_{r,\tau_r(M_r-2)}} \\ \gamma_{m_{r,M_r-1}} &= \alpha'_{m_{r,\tau_r(M_2)}} \end{cases} \quad (\text{A6})$$

This shows that trivial cross-homology classes in $H_{0,0}^{(1)}(X)$ are given by cross-cycles obtained from cross-chains on kites; that is images of sums of cross-chains in the form of (A1). \square

Appendix B: Hodge Theory

1. Harmonic cross-forms as cross-homology classes

Let

$$\mathcal{L}_{k,l}^{(\text{TO})} := (\delta_{k,l}^{(1)})^* \delta_{k,l}^{(1)}, \quad \mathcal{L}_{k,l}^{(\text{TI})} := \delta_{k-1,l}^{(1)} (\delta_{k-1,l}^{(1)})^*,$$

and

$$\mathcal{L}_{k,l}^{(\text{BO})} := (\delta_{k,l}^{(2)})^* \delta_{k,l}^{(2)}, \quad \mathcal{L}_{k,l}^{(\text{BI})} := \delta_{k-1,l}^{(2)} (\delta_{k-1,l}^{(2)})^*,$$

so that

$$\mathcal{L}_{k,l}^{(\text{T})} := \mathcal{L}_{k,l}^{(\text{TO})} + \mathcal{L}_{k,l}^{(\text{TI})},$$

and

$$\mathcal{L}_{k,l}^{(\text{B})} := \mathcal{L}_{k,l}^{(\text{BO})} + \mathcal{L}_{k,l}^{(\text{BI})}.$$

We denote the spaces of harmonic cross-forms on X as

$${}^{(s)}\mathcal{H}_{k,l} = \ker \mathcal{L}_{k,l}^{(s)} = \{\phi \in C^{k,l} \mid \mathcal{L}_{k,l}^{(s)} \phi = 0\}, s = T, B$$

Then, we have the following group isomorphisms generalizing [7, 15].

Lemma B.1. For $s = 1, 2$ and for all $k, l \geq -1$, we have

$$H_{k,l}^{(s)}(X) \cong \ker(\mathcal{L}_{k,l}^{(s)}), \quad (\text{B1})$$

where we have used the notations $\mathcal{L}_{k,l}^{(1)} = \mathcal{L}_{k,l}^{(\text{T})}$ and $\mathcal{L}_{k,l}^{(2)} = \mathcal{L}_{k,l}^{(\text{B})}$.

Proof. Let's prove this result for $s = 1$ (similar arguments apply to $s = 2$). First, notice that from the identification $C_{k,l} = C^{k,l}$ we obtain

$$H_{k,l}^{(1)}(X) = \ker(\delta_{k,l}^{(1)}) / \text{im}(\delta_{k-1,l}^{(1)}) \cong \ker(\delta_{k,l}^{(1)}) \cap \text{im}(\delta_{k-1,l}^{(1)})^\perp, \quad (\text{B2})$$

and as the analog holds for $H_{(2)}^{k,l}(X)$. Moreover, recall from linear algebra that if $E \xrightarrow{f} F$ is a linear operator on two vector spaces equipped with inner products, then $\ker(f^* f) = \ker f$. Indeed, we clearly have $\ker f \subset \ker(f^* f)$. Next, if $x \in \ker(f^* f)$, then $\langle f^* f x, y \rangle_E = \langle f x, f y \rangle_F = 0$ for all $y \in E$, which implies that $x \in \ker f$. In our case we have $\delta_{k,l}^{(1)} \delta_{k-1,l}^{(1)} = 0$ and $(\delta_{k-1,l}^{(1)})^* (\delta_{k,l}^{(1)})^* = 0$; hence

$$\begin{aligned} \text{im}(\mathcal{L}_{k,l}^{(\text{TO})}) &\subset \text{im}(\delta_{k,l}^{(1)})^* \subset \ker(\delta_{k-1,l}^{(1)})^* \subset \ker(\delta_{k-1,l}^{(1)} (\delta_{k-1,l}^{(1)})^*) \\ \text{im}(\mathcal{L}_{k,l}^{(\text{TI})}) &\subset \text{im}(\delta_{k-1,l}^{(1)}) \subset \ker(\delta_{k,l}^{(1)}) \subset \ker((\delta_{k,l}^{(1)})^* \delta_{k,l}^{(1)}). \end{aligned}$$

Therefore

$$\begin{aligned} \ker \mathcal{L}_{k,l}^{(\text{T})} &= \ker((\delta_{k,l}^{(1)})^* \delta_{k,l}^{(1)}) \cap \ker(\delta_{k-1,l}^{(1)} (\delta_{k-1,l}^{(1)})^*) \\ &= \ker(\delta_{k,l}^{(1)}) \cap \ker(\delta_{k-1,l}^{(1)})^* \\ &\cong \ker(\delta_{k,l}^{(1)}) \cap \text{im}(\delta_{k-1,l}^{(1)})^\perp, \end{aligned}$$

and the isomorphism (B1) follows from (B2). \square

It follows that the eigenvectors corresponding to the zero eigenvalue of the (k, l) -cross-Laplacian $\mathcal{L}_{k,l}^{(s)}$ are representative cross-cycles in the homology group $H_{k,l}^{(s)}(X)$. Henceforth, we see that in order to get the dimensions of the cross-homology groups $H_{k,l}^{(s)}(X)$, it suffices to find the eigenspaces corresponding to the zero eigenvalues of $\mathcal{L}_{k,l}^{(s)}$. That is,

$$\beta_{k,l}^{(1)} = \dim \ker \mathcal{L}_{k,l}^{(1)}, \text{ and } \beta_{k,l}^{(2)} = \dim \ker \mathcal{L}_{k,l}^{(2)}. \quad (\text{B3})$$

2. Matrix representations of the cross-Laplacians

In order to compute these matrix representations of the (k, l) -cross-Laplacians, we first need to give their formal expressions as linear operators. Thanks to (9), we get for $\phi \in C^{k,l}$ and $a \in X_{k,l}$:

$$\begin{aligned} (\delta_{k,l}^{(1)})^* \delta_{k,l}^{(1)} \phi([a]) &= \sum_{\substack{a' \in X_{k+1,l} \\ a \in \partial^{(1)} a'}} \frac{w(a')}{w(a)} \operatorname{sgn}(a, \partial^{(1)} a) (\delta_{k,l}^{(1)} \phi)([a']) \\ &= \sum_{\substack{a' \in X_{k+1,l} \\ a \in \partial^{(1)} a'}} \frac{w(a')}{w(a)} \operatorname{sgn}(a, \partial^{(1)} a') \sum_{b \in \partial^{(1)} a'} \operatorname{sgn}(b, \partial^{(1)} a') \phi([b]) \\ &= \sum_{\substack{a' \in X_{k+1,l} \\ a \in \partial^{(1)} a'}} \frac{w(a')}{w(a)} \operatorname{sgn}(a, \partial^{(1)} a') \left[\operatorname{sgn}(a, \partial^{(1)} a') \phi([a]) + \sum_{b \in \partial^{(1)} a', b \neq a} \operatorname{sgn}(b, \partial^{(1)} a') \phi([b]) \right] \\ &= \sum_{\substack{a' \in X_{k+1,l} \\ a \in \partial^{(1)} a'}} \frac{w(a')}{w(a)} \left[\phi([a]) + \sum_{b \in \partial^{(1)} a', a \neq b} \operatorname{sgn}(a, \partial^{(1)} a') \operatorname{sgn}(b, \partial^{(1)} a') \phi([b]) \right], \end{aligned}$$

and

$$\begin{aligned} \delta_{k-1,l}^{(1)} (\delta_{k-1,l}^{(1)})^* \phi([a]) &= \sum_{\substack{c \in X_{k-1,l} \\ c \in \partial^{(1)} a}} \operatorname{sgn}(c, \partial^{(1)} a') \sum_{\substack{a' \in X_{k,l} \\ c \in \partial^{(1)} a'}} \frac{w(a')}{w(c)} \operatorname{sgn}(c, \partial^{(1)} a') \phi([a']) \\ &= \sum_{\substack{c \in X_{k-1,l} \\ c \in \partial^{(1)} a}} \operatorname{sgn}(c, \partial^{(1)} a) \left[\frac{w(a)}{w(c)} \operatorname{sgn}(c, \partial^{(1)} a) \phi([a]) \right. \\ &\quad \left. + \sum_{\substack{c \in \partial^{(1)} a' \\ a \neq a'}} \frac{w(a')}{w(c)} \operatorname{sgn}(c, \partial^{(1)} a') \phi([a']) \right] \\ &= \sum_{\substack{c \in X_{k-1,l} \\ c \in \partial^{(1)} a}} \frac{w(a)}{w(c)} \phi([a]) + \sum_{\substack{c \in X_{k-1,l}, a' \in X_{k,l} \\ c \in \partial^{(1)} a' \cap \partial^{(1)} a}} \frac{w(a')}{w(c)} \operatorname{sgn}(c, \partial^{(1)} a) \operatorname{sgn}(c, \partial^{(1)} a') \phi([a']). \end{aligned}$$

In particular, when ϕ is an elementary cross-form e_b , $b \in X_{k,l}$, we get

$$\mathcal{L}_{k,l}^{(TO)} e_b([a]) = \begin{cases} \frac{1}{w(a)} \deg_{TO}(a), & \text{if } a = b, \\ -\frac{w(c)}{w(a)}, & \text{if } a \neq b \text{ and } a \frown_c^{(1)} b, \\ & \text{and } \text{sgn}(a) = \text{sgn}(b), \\ \frac{w(c)}{w(a)}, & \text{if } a \neq b \text{ and } a \frown_c^{(1)} b, \\ & \text{and } \text{sgn}(a) = -\text{sgn}(b), \\ 0, & \text{otherwise,} \end{cases} \quad \text{and } \mathcal{L}_{k,l}^{(TI)} e_b([a]) = \begin{cases} w(a) \deg_{TI}(a), & \text{if } a = b, \\ \frac{w(b)}{w(d)}, & \text{if } a \neq b \text{ and } a \smile_{(1)}^d b, \\ & \text{and } \text{sgn}(a) = \text{sgn}(b), \\ -\frac{w(b)}{w(d)}, & \text{if } a \neq b \text{ and } a \smile_{(1)}^d b \\ & \text{and } \text{sgn}(a) = -\text{sgn}(b), \\ 0, & \text{otherwise.} \end{cases}$$

It follows that the (a, b) -th entry of the matrix representation of the top (k, l) -cross-Laplacian $\mathcal{L}_{k,l}^{(T)}$ with respect to the

inner product defined from the weight w on X is given by

$$(\mathcal{L}_{k,l}^{(T)})_{a,b} = \begin{cases} \frac{1}{w(a)} \deg_{TO}(a) + w(a) \deg_{TI}(a), & \text{if } a = b, \\ \frac{w(b)}{w(d)} - \frac{w(c)}{w(a)}, & \text{if } a \neq b, a \frown_c^{(1)} b, a \smile_{(1)}^d b, \\ & \text{and } \text{sgn}(a) = \text{sgn}(b), \\ \frac{w(c)}{w(a)} - \frac{w(b)}{w(d)}, & \text{if } a \neq b, a \frown_c^{(1)} b, a \smile_{(1)}^d b, \\ & \text{and } \text{sgn}(a) = -\text{sgn}(b), \\ \frac{w(b)}{w(d)}, & \text{if } a \neq b, a \smile_{(1)}^d b, \text{sgn}(a) = \text{sgn}(b), \\ & \text{and not top - outer adjacent,} \\ -\frac{w(b)}{w(d)}, & \text{if } a \neq b, a \smile_{(1)}^d b, \text{sgn}(a) = -\text{sgn}(b), \\ & \text{and not top - outer adjacent,} \\ 0, & \text{otherwise.} \end{cases} \quad (\text{B4})$$

And it is clear that we get similar matrix representation for

the bottom (k, l) -cross-Laplacian $\mathcal{L}_{k,l}^{(B)}$.

- [1] A. R. Benson, R. Abebe, M. T. Schaub, A. Jadbabaie, and J. M. Kleinberg. Simplicial closure and higher-order link prediction. *Proceedings of the National Academy of Sciences*, 115:E11221 – E11230, 2018.
- [2] A. R. Benson, D. F. Gleich, and J. Leskovec. Higher-order organization of complex networks. *Science*, 353(6295):163–166, 2016.
- [3] G. Bianconi. *Higher-order networks*. Cambridge University Press, 2021.
- [4] S. Boccaletti, G. Bianconi, R. Criado, C. I. Del Genio, J. Gómez-Gardenes, M. Romance, I. Sendina-Nadal, Z. Wang, and M. Zanin. The structure and dynamics of multilayer networks. *Physics reports*, 544(1):1–122, 2014.
- [5] A. Cardillo, J. Gómez-Gardenes, M. Zanin, M. Romance, D. Papo, F. d. Pozo, and S. Boccaletti. Emergence of network features from multiplexity. *Scientific reports*, 3(1):1–6, 2013.
- [6] M. De Domenico, A. Solé-Ribalta, E. Cozzo, M. Kivela, Y. Moreno, M. A. Porter, S. Gómez, and A. Arenas. Mathematical formulation of multilayer networks. *Physical Review X*, 3(4):041022, 2013.
- [7] B. Eckmann. Harmonische funktionen und randwertaufgaben in einem komplex. *Commentarii Mathematici Helvetici*, 17:240–255, 1944.
- [8] J. Flores and M. Romance. On eigenvector-like centralities for temporal networks: Discrete vs. continuous time scales. *Journal of Computational and Applied Mathematics*, 330:1041–1051, 2018.
- [9] S. Fortunato and D. Hric. Community detection in networks: A user guide. *Physics reports*, 659:1–44, 2016.
- [10] R. Ghorbanchian, J. G. Restrepo, J. J. Torres, and G. Bianconi. Higher-order simplicial synchronization of coupled topological signals. *Communications Physics*, 4(1):120, 2021.
- [11] C. Giusti, E. Pastalkova, C. Curto, and V. Itskov. Clique topology reveals intrinsic geometric structure in neural correlations. *Proceedings of the National Academy of Sciences*, 112(44):13455–13460, 2015.
- [12] P. G. Goerss and J. F. Jardine. *Simplicial homotopy theory*. Springer Science & Business Media, 2009.
- [13] A. Griffa, B. Ricaud, K. Benzi, X. Bresson, A. Daducci, P. Vandergheynst, J.-P. Thiran, and P. Hagmann. Transient networks

- of spatio-temporal connectivity map communication pathways in brain functional systems. *NeuroImage*, 155, 04 2017.
- [14] A. Hatcher. *Algebraic topology*. Cambridge Univ. Press, Cambridge, 2000.
- [15] D. Horak and J. Jost. Spectra of combinatorial laplace operators on simplicial complexes. *Advances in Mathematics*, 244:303–336, 2013.
- [16] I. Iacopini, G. Petri, A. Barrat, and V. Latora. Simplicial models of social contagion. *Nature communications*, 10(1):2485, 2019.
- [17] M. Kivelä, A. Arenas, M. Barthelemy, J. P. Gleeson, Y. Moreno, and M. A. Porter. Multilayer networks. *Journal of complex networks*, 2(3):203–271, 2014.
- [18] S. Lane. *Homology*. Grundlehren der mathematischen Wissenschaften in Einzeldarstellungen mit besonderer Berücksichtigung der Anwendungsgebiete. Academic Press, 1963.
- [19] L.-H. Lim. Hodge laplacians on graphs. *SIAM Review*, 62, 07 2015.
- [20] X. Liu, E. Maiorino, A. Halu, K. Glass, R. B. Prasad, J. Loscalzo, J. Gao, and A. Sharma. Robustness and lethality in multilayer biological molecular networks. *Nature Communications*, 11(1):6043, 2020.
- [21] Q. F. Lotito, F. Musciotto, A. Montresor, and F. Battiston. Higher-order motif analysis in hypergraphs. *Communications Physics*, 5(1):79, 2022.
- [22] M. Lucas, G. Cencetti, and F. Battiston. Multiorder laplacian for synchronization in higher-order networks. *Physical Review Research*, 2(3):033410, 2020.
- [23] S. Majhi, M. Perc, and D. Ghosh. Dynamics on higher-order networks: A review. *Journal of the Royal Society Interface*, 19(188):20220043, 2022.
- [24] K. Mandke, J. Meier, M. J. Brookes, R. D. O’Dea, P. Van Mieghem, C. J. Stam, A. Hillebrand, and P. Tewarie. Comparing multilayer brain networks between groups: Introducing graph metrics and recommendations. *NeuroImage*, 166:371–384, 2018.
- [25] I. Moerdijk. *Bisimplicial Sets and the Group-Completion Theorem*, pages 225–240. Springer Netherlands, Dordrecht, 1989.
- [26] M. E. Newman. The structure and function of complex networks. *SIAM review*, 45(2):167–256, 2003.
- [27] M. Pedersen, A. Zalesky, A. Omidvarnia, and G. D. Jackson. Multilayer network switching rate predicts brain performance. *Proceedings of the National Academy of Sciences*, 115(52):13376–13381, 2018.
- [28] S. Pilosof, M. A. Porter, M. Pascual, and S. Kéfi. The multilayer nature of ecological networks. *Nature Ecology & Evolution*, 1(4):0101, 2017.
- [29] J. Rotman. *An Introduction to Homological Algebra*. Universitext. Springer New York, 2008.
- [30] R. J. Sánchez-García, E. Cozzo, and Y. Moreno. Dimensionality reduction and spectral properties of multilayer networks. *Physical Review E*, 89(5):052815, 2014.
- [31] M. T. Schaub, A. R. Benson, P. Horn, G. Lippner, and A. Jadbabaie. Random walks on simplicial complexes and the normalized hodge 1-laplacian. *SIAM Review*, 62(2):353–391, 2020.
- [32] D. Shi, Z. Chen, X. Sun, Q. Chen, C. Ma, Y. Lou, and G. Chen. Computing cliques and cavities in networks. *Communications Physics*, 4, 11 2021.
- [33] L. Solá Conde, M. Romance, R. Herrero, J. Flores, A. García del Amo, and S. Boccaletti. Eigenvector centrality of nodes in multiplex networks. *Chaos (Woodbury, N.Y.)*, 23:033131, 09 2013.
- [34] S. Timóteo, M. Correia, S. Rodríguez-Echeverría, H. Freitas, and R. Heleno. Multilayer networks reveal the spatial structure of seed-dispersal interactions across the great rift landscapes. *Nature Communications*, 9(1):140, 2018.
- [35] E. Vasilyeva, A. Kozlov, K. Alfaro, D. Musatov, A. Raigorodskii, M. Perc, and S. Boccaletti. Multilayer representation of collaboration networks with higher-order interactions. *Scientific Reports*, 11:5666, 03 2021.
- [36] M. Wu, S. He, Y. Zhang, J. Chen, Y. Sun, Y.-Y. Liu, J. Zhang, and H. V. Poor. A tensor-based framework for studying eigenvector multicentrality in multilayer networks. *Proceedings of the National Academy of Sciences*, 116:15407 – 15413, 2019.
- [37] J. Xu, T. L. Wickramaratne, and N. V. Chawla. Representing higher-order dependencies in networks. *Science advances*, 2(5):e1600028, 2016.
- [38] H. Yin, A. R. Benson, and J. Leskovec. Higher-order clustering in networks. *Physical Review E*, 97(5):052306, 2018.
- [39] J.-G. Young, G. Petri, and T. P. Peixoto. Hypergraph reconstruction from network data. *Communications Physics*, 4(1):135, 2021.
- [40] M. Yuvaraj, A. K. Dey, V. Lyubchich, Y. R. Gel, and H. V. Poor. Topological clustering of multilayer networks. *Proceedings of the National Academy of Sciences*, 118(21), 2021.